R. Song, D. Ponge, R. Kaspar, D. Raabe
Max-Planck-Institut für Eisenforschung, Düsseldorf, Germany

Grain boundary characterization and grain size measurement in an ultrafine-grained steel

Dedicated to Professor Dr. Peter Neumann on the occasion of his 65th birthday

Ultrafine ferrite grains in a plain C–Mn steel (0.3 mass% C) were produced by large-strain warm compression and subsequent annealing treatment in a temperature range between 773 K and 1003 K. The samples were investigated by means of high-resolution electron back-scatter diffraction. The resulting microstructures showed very fine ferrite grains and homogeneously distributed cementite particles. The majority of the grain boundaries (55–70 %) were classified as high-angle ones (≥ 15° misorientation). When considering only these high-angle grain boundaries, the average grain size changed from 0.9 µm at a deformation temperature of 773 K to 2.2 µm at a deformation temperature of 1003 K. For the same range the average subgrain sizes increased from 0.6 µm to 1.5 µm. The basic result of this study is that the grain size characterization of polycrystalline microstructures with ultrafine grains requires the use of the high-resolution electron back-scatter diffraction method in conjunction with a careful analysis of the grain boundary character.

Keywords: Steel; Texture; Ultrafine-grained microstructure; Grain size; EBSD; Misorientation

1. Introduction

1.1. Grain size and grain boundary characterization in ultrafine-grained steel

Grain refinement is an effective method to improve strength and toughness simultaneously without addition of alloying elements. In general, the term 'ultrafine grain' is used to define microstructures with grain sizes between 100 nm and 1000 nm, whereas the term 'nano structure' refers to grain sizes below 100 nm. In order to obtain ultrafine grains in steels, several new concepts have been proposed at the laboratory and pilot-plant scale, such as large-strain reduction (strain-induced ferrite transformation), between Ae_3 and Ar_3[1] multi-axial deformation, equal channel angular pressing or extrusion (ECAP/ECAE) and deformation under a high magnetic field [1–7]. Among these approaches, severe plastic deformation with a true logarithmic strain, ε, above 1.0 at low homologous temperature (usually less than 0.3–0.4 T_m) is commonly accepted as the most efficient way to obtain ultrafine-grained steel with a ferrite grain size in the range of 0.3–2.0 µm when it comes to large-scale processing approaches. However, in most investigations on this topic it is unclear if the published grain size measures refer to an average crystal size which derives from counting *exclusively* high-angle grain boundaries or from counting *both*, high-angle and low-angle grain boundaries without distinction. Differentiation between the two, however, is of substantial importance since large-strain thermomechanical processing of high-stacking fault metals typically entails microstructures which contain a substantial fraction of low-angle subgrain segments relative to all grain boundaries. Besides this basic crystallographic issue, careful investigation of the fraction of low-angle grain boundaries in a thermomechanically treated steel can help to investigate two important questions which are related to this aspect. First, quantification of the grain boundary character distribution is required to track and understand the competition between recovery and subgrain coarsening on the one hand (entailing primarily low-angle subgrain structures) and primary recrystallization on the other hand (entailing essentially high-angle grain structures). As mentioned above, steels with ultrafine microstructures are produced – when it comes to large sample sizes (in the kg range and above) – by severe plastic deformation in conjunction with a thermal treatment. Such processing routes naturally involve the whole complexity of static and dynamic recovery and recrystallization processes. Therefore, the knowledge of the grain boundary character distribution is of great value to separate these mechanisms from each other [8–10]. Second, grain boundary characterization is necessary to clearly identify the mechanisms which govern the mechanical properties of such steels. One aspect in this context is, for instance, the validity of the Hall–Petch relationship in ultrafine-grained steels (with an average grain size below 500 nm).

Before starting to determine grain sizes in the light of these aspects, for instance by using high-resolution electron back-scatter diffraction (EBSD), it is at first necessary to properly define the meaning of the term 'grain'. This is not a trivial task because in ultrafine-grained steels which are formed by large-strain thermomechanical treatment one can observe [11] that crystalline entities (grains) can be bordered both, by high-angle grain boundary segments with misorientations above 15° and at the same time by low-angle grain boundary segments with misorientations below 15°. An obvious sensible way to define the grain size in this context is the distinction between low- and high-angle

[1] Ae_3: equilibrium austenite-to-ferrite transformation temperature, Ar_3: austenite-to-ferrite transformation temperature during cooling.

© 2004 Carl Hanser Verlag, Munich, Germany www.hanser.de/mk Not for use in internet or intranet sites. Not for electronic distribution.

TRIAL MODE − a valid license will remove this message. See the keywords property of this PDF for more information.

Applied

© 2004 Carl Hanser Verlag, Munich, Germany www.hanser.de/mk Not for use in internet or intranet sites. Not for electronic distribution.

boundary segments owing to their different capability to act as barriers to crack propagation and continuous dislocation flow [12–19]. In micromechanical terms this means to define the grain size as a '*mechanically relevant grain size*', where the crystal borders are predominantly formed by high-angle grain boundaries. Especially when considering the toughness of steels, low-angle grain boundaries are known to be less effective in impeding crack growth than high-angle grain boundaries. This means that steel crystals which are separated by a low-angle grain boundary can be regarded as a single entity in micromechanical terms.

1.2. Related previous work on ultrafine grain size analysis

High-resolution EBSD methods can serve to resolve orientational grain boundary details above 0.5° [16–19]. Such an approach also allows one to scan and quantify large numbers of grains and subgrains (above 0.5°) in order to obtain good statistics. In the following we give a concise review of some recent related studies on grain boundary characterization in ultrafine grain microstructures on the basis of high-resolution EBSD analysis [12, 13, 15–16].

Kim et al. [12] suggested to quantify the effective grain size (equivalent to the '*mechanically relevant grain size*' introduced above) in bainitic steels from the viewpoint of the misorientation. They suggested that grains which reveal in 2D sections adjacent grain boundary segments with misorientations above 15° should be regarded as "high-angle grains" and should be correspondingly counted in the calculation of the effective grain size. The effective grain size which was calculated by this method matched well with the size of the facets which appeared in the fracture surfaces.

Wang et al. [20] studied grain growth in an Al-3 % Mg alloy during annealing for various times at 473 K after an ECAP process. For determining the growth rates the authors measured the mean linear grain boundary intercept lengths of recovered and unrecovered grains by use of TEM maps after each annealing step. By using high-resolution EBSD analysis, Gholinia et al. [15] studied the formation of submicron grain structures processed by ECAE in an Al-3 %Mg sample. The authors analysed the fraction of high-angle grain boundaries and the sizes of grains and subgrains which were observed within the large grains. Gholinia et al. [17] studied by high-resolution EBSD the grain structures which developed in two Al-3 %Mg alloys by continuous recrystallization during rolling. They found that the spacing between high-angle grain boundaries, as observed in the EBSD maps perpendicular to the rolling direction, was similar to the subgrain size after a true strain of about 2. Park and Shin [21] investigated the evolution of submicron-sized grains in a low-carbon steel processed by ECAP during annealing. The authors used the average values of the linear intercept size measured from 7 to 10 TEM dark field images for each microstructural state as a measure for the grain size.

The quoted studies show that the high-resolution SEM–EBSD technique is widely accepted as a quantitative characterization tool for grain size determination in ultrafine-grained material. The investigations reveal that it is possible to determine some average measure for the grain size by the high-resolution EBSD technique. However, it is also apparent that in some of these studies no clear distinction has been made between grains and subgrains. This means that the obtained data cannot be directly used to calculate those mechanical properties of the respective samples which depend on the high-angle character of the grain size. Hence, microstructure–property relationships based on physical principles cannot be established in such cases. Those studies which treated this aspect in more detail by separating (high-angle) grain sizes from subgrains typically used the mean linear intercept method in combination with TEM mappings. Despite the high quality of such an approach it is less suited in the current case since the areas which one can investigate by TEM are too small for a systematic quantitative study on the grain size in thermomechanically treated steels. Another important reason for the current study is the fact that most of the previous work along these lines was conducted on Al alloys.

The present investigation is a quantitative study on grain size characterization in deformed and annealed plain C–Mn steels with grain sizes in the micron and submicron regime. For this purpose we use EBSD analysis in conjunction with a high-resolution field-emission gun scanning electron microscope (FEGSEM). The analysis is conducted by using a mean linear intercept method which is capable of properly separating grains from subgrains.

2. Experimental methods

2.1. Specimens and thermomechanical treatment

A C–Mn steel of the composition given in Table 1 was melted in a laboratory vacuum induction furnace. The cast ingot had a weight of 70 kg and a size of 140 mm × 140 mm × 300 mm (width × length × height). The laboratory samples were machined directly from the ingot into cylindrical specimens (5 mm × 10 mm (diameter × length)) for dilatometry, and into rectangular parallelepiped samples (18 mm × 18 mm × 30 mm (weight × length × height)) for hot compression tests which were conducted in a set-up with a maximum force of 2.5 MN [23]. This servohydraulic press is capable of conducting large-scale thermomechanical processes by performing multi-step hot compression tests as a realistic approximation of industry-scale hot-forming operations.

Since the refinement of the austenite is essential for obtaining small grains after transformation, the experiments were in all cases carried out with a low austenitization and austenite deformation temperature. The reheating temperature (T_{rh}) was 1173 K, i. e., 100 K above A_3. Austenite deformation was conducted at 1143 K to a true logarithmic strain of $\varepsilon = 0.3$ at a strain rate of 10 s^{-1}. The sample was exposed to water quenching immediately after the deformation in order to study the resulting austenite structure. We studied cooling rates in the range between 2 Ks^{-1} and 64 Ks^{-1} in order to establish a continuous cooling transformation diagram (DCCT).

Steel microstructures consisting of small-grained ferrite and a fine dispersion of cementite are known to provide

Table 1. Chemical composition (mass%), A_3 calculated by Thermo-Calc [22].

Fe	C	Si	Mn	P	S	Al	N	A_3
balance	.31	.22	.76	.003	.003	.030	.001	1071 K

TRIAL MODE − a valid license will remove this message. See the keywords property of this PDF for more information.

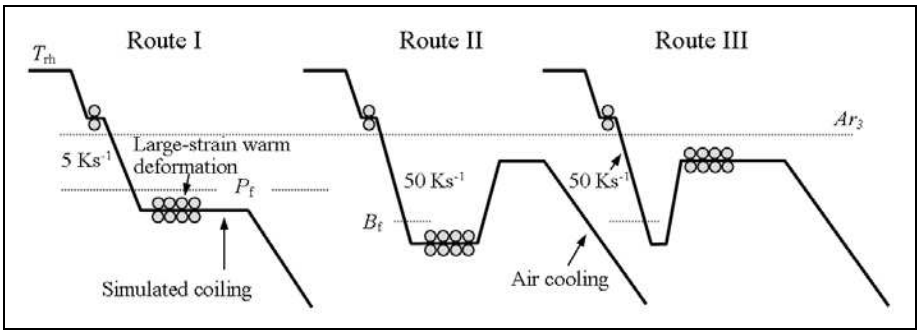

Fig. 1. Processing schedules for the compression tests. T_{rh}: Reheating temperature; Ar_3: Austenite-to-ferrite transformation temperature; P_f: Pearlite finish temperature; B_f: Bainite finish temperature.

good mechanical properties. Therefore, large-strain warm deformation was applied below the $\gamma \rightarrow \alpha$ transformation in order to refine the ferrite and to spheroidize the cementite. In route I (Fig. 1) a cooling rate of 5 Ks^{-1} after austenite deformation provided a fine ferrite plus pearlite microstructure prior to large-strain multi-step warm deformation. After holding the samples for 2 min, four deformation steps (uniaxial symmetrical compression) were exerted in the temperature range between 773 K and 973 K. Each of the four subsequent passes imposed a true strain of $\varepsilon = 0.4$ at a strain rate of 10 s^{-1}, accumulating to a total strain of $\varepsilon = 1.6$. Subsequently, an isothermal treatment of 2 h was imposed in order to mimic coiling conditions.

In routes II and III (Fig. 1) a bainitic microstructure was produced by using a cooling rate of 50 Ks^{-1} after deformation in the austenite regime. This treatment provided the starting microstructure for the subsequent large-strain deformation. In route II, severe plastic deformation was performed below the bainite finish temperature (B_f). In order to obtain a recrystallized ferrite microstructure containing homogeneously distributed cementite particles, the material was reheated after large-strain deformation to different temperature levels in the range between 773 K and 1003 K using a holding time of 2 h to approximate coiling conditions. In route III, the material was first reheated to the respective deformation temperatures in the range between 823 K and 1003 K. Coiling was simulated by holding the samples for 2 h at the deformation temperature.

2.2. Microstructure characterization and grain size determination

The specimens were cut parallel to the compression direction (CD) for optical metallography using a 1 % nital solution for etching. Micrographs were taken at sample locations where the local strain was equal to the nominal strain according to finite element calculations.

The samples were also studied using high-resolution electron backscatter diffraction. The measurements were conducted on a JSM–6500F field emission scanning electron microscope at an accelerating voltage of 15 kV and an emission current of about 100 nA. Crystallographic orientation mappings were taken using a step size of 100 nm in an area of 50 µm × 50 µm on the same samples which were used for optical metallography. About 300 000 orientation points were analysed for each mapping. In the analysis of the texture mappings we count interfaces with a misorientation above 15° as high-angle grain boundaries. Boundaries with misorientations in the range between 2° and 15° are recorded as low-angle grain boundaries. Interfaces with misorientations below 2° were ignored in the analysis because of the limits set by the orientation measurement and by the lateral resolutions of the mappings.

Ultrafine grains in steels are often not entirely bordered by high-angle boundaries, i. e., some of the grain boundary segments may have low-angle character. For this reason we extracted the grain diameters from the EBSD maps along CD and along the transverse direction (TD) of the samples. The grain sizes were then defined as the average diameter of circles which have an area equivalent to that of an average elliptical-shaped grain. The grain shape aspect ratio providing the ellipsoidal form was defined as the mean linear intercept in TD divided by that in CD. The sizes of the cementite particles were also determined by the mean linear intercept method from SEM micrographs.

3. Experimental results and discussion

The microstructures obtained for the three processing schemes are similar, i. e., they consist of ferrite with a small grain size and globular cementite particles. The microstructure for route III is shown as an SEM image (Fig. 2a) and EBSD map (Fig. 2b). The microstructure obtained for a heat treatment above 913 K reveals an equiaxed shape. Lower temperatures lead to finer ferrite grains and cementite particles (5 nm–350 nm), but the grain shape is more elongated than that after 973 K. An increase in the deformation temperature results in coarser and more equiaxed ferrite grains. The distribution of cementite particles tends to be more homogeneous and the particle size becomes larger (250–950 nm) at temperatures above 973 K.

Fig. 2b represents the EBSD maps from the same samples as shown in Fig. 2a. The maps show the image quality index (IQ) of the pseudo-Kikuchi lines together with the grain boundaries. Black lines indicate misorientations above 15° between adjacent points, i. e., they represent high-angle grain boundary segments. The white lines indicate misorientations between 2 and 15°. The white spots at the grain boundary triple points visible in the map taken on the sample treated at 973 K are cementite particles with sizes in the range between 300 nm and 950 nm, i. e., they are larger than the step size (100 nm) of the EBSD measurement.

Fig. 3 shows the fraction of high-angle grain boundaries for the three processing routes. For the different deformations (routes I and III) and annealing temperatures (route II) ranging from 773 K to 973 K, the fraction of high-angle grain boundaries remains between 55 % and 70 %. A detailed analysis of the grain boundary maps, though, reveals that many grains are bordered by both, high- and low-angle grain boundaries.

© 2004 Carl Hanser Verlag, Munich, Germany www.hanser.de/mk Not for use in internet or intranet sites. Not for electronic distribution.

TRIAL MODE − a valid license will remove this message. See the keywords property of this PDF for more information.

Applied

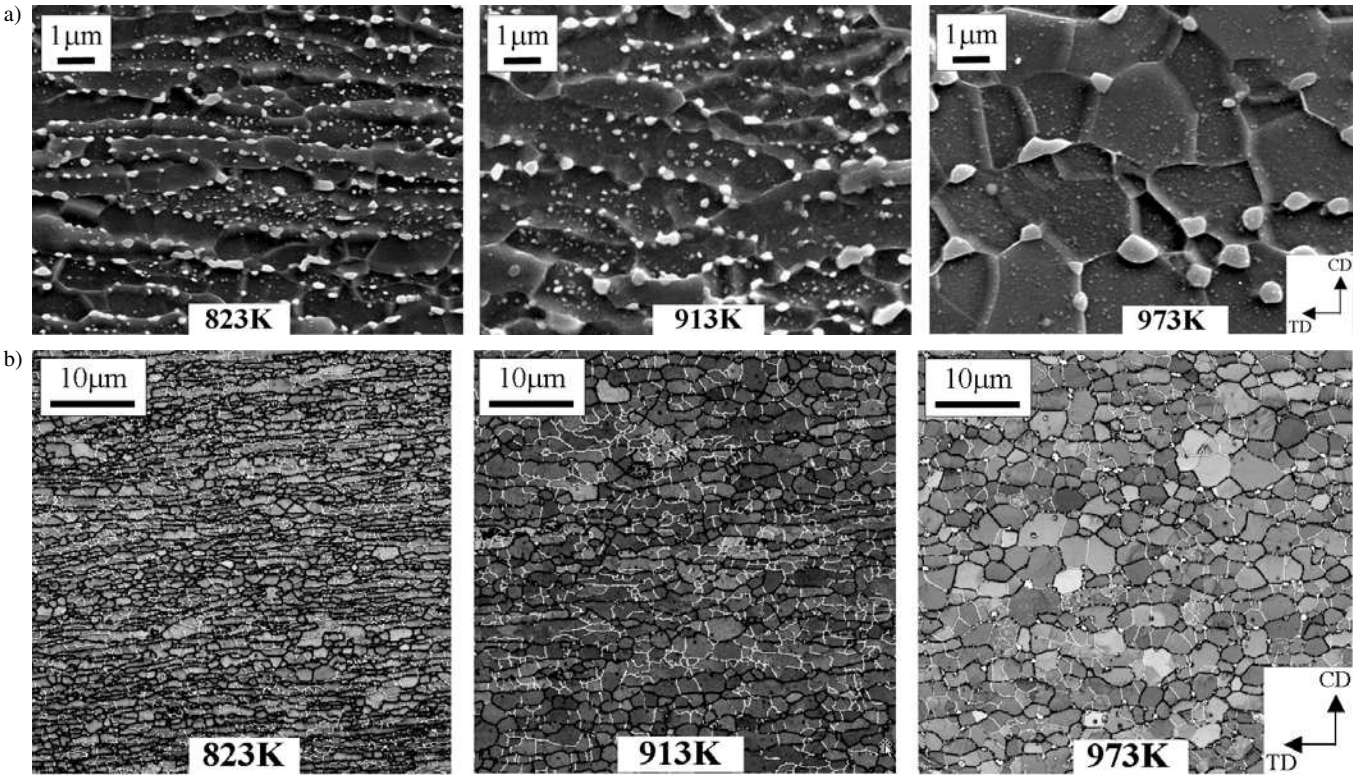

Fig. 2. SEM images (a) and EBSD maps (b) after large-strain deformation ($\varepsilon = 1.6$) and subsequent 2 h annealing at different temperatures. Details of the processing are given in Fig. 1 (CD: compression direction; TD: transverse direction). The black lines indicate grain boundary misorientations between 15° and 63°. White lines indicate grain boundary misorientations between 2° and 15°.

Fig. 4 shows the grain sizes together with the grain shape aspect ratios as obtained for route III from the EBSD map analysis. The data reveal true (high-angle) grain sizes in the range between 1 µm and 2 µm (Fig. 4a). The aspect ratio for these *mechanically relevant* grains amounts to 2 for the low-temperature regime and drops to 1.5 for higher temperatures. The true (low-angle) subgrains (Fig. 4c) reveal a constant aspect ratio of about 1.1. It is important to note that the aspect ratio of the subgrains is independent of the temperature while their absolute size increases from about 2 µm to 3 µm as the temperature increases from 773 K to 973 K.

Fig. 5 shows the corresponding average data for the grain shape aspect ratio for all process routes. All grains and subgrains (except for the subgrains obtained for route III) are elongated perpendicularly to the compression direction at low temperatures, but more equiaxed at high temperatures. For route II the aspect ratio of the grains and subgrains almost drops by a factor of two. The material contained a uniform dispersion of fine cementite particles (with an average size below 250 nm) which may be the cause for a strong inhibition of grain boundary migration in terms of Zener pinning, thereby effectively preserving a deformation grain shape.

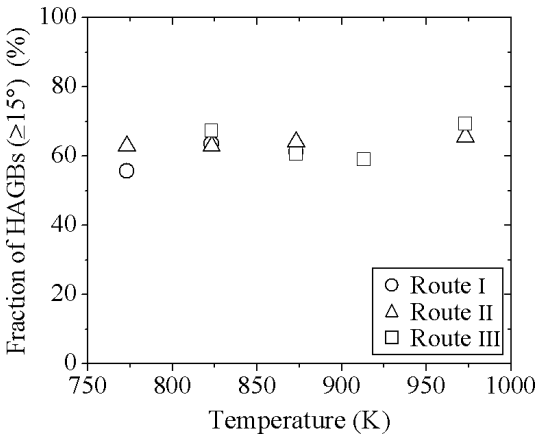

Fig. 3. Fraction of high-angle grain boundaries (LAGB) obtained for the three different processing routes (see details of processing in Fig. 1).

Higher temperatures above 873 K lead to faster diffusion and Ostwald ripening of the cementite particles. Particles above 300 nm are known in steels as weak obstacles to the capillary-driven motion of the ferrite grain boundaries so that higher temperatures entail more equiaxed grain shapes of the ferrite.

In comparison to alternative routes producing an ultrafine single phase ferritic and lamellar pearlitic microstructure, the present results which show a uniform dispersion of cementite particles in a fine ferrite matrix are advantageous, since such microstructures increase strain hardening and reduce the tendency for plastic instabilities. This important in particular if the grain size of the ferrite is very small [16]. The increase in strain hardening can be attributed to an increase in the rate of dislocation multiplication at particles and to the decrease of the mean free path of dislocations.

While conventional approaches use quenching and a tempering heat treatment to obtain fine carbide particles distributed homogenously in the ferritic matrix [16], our study pursued a large-strain warm-deformation strategy below the $\gamma \rightarrow \alpha$ transformation temperature of a ferrite plus pearlite or a bainitic microstructure, respectively, for reaching the same aim.

© 2004 Carl Hanser Verlag, Munich, Germany www.hanser.de/mk Not for use in internet or intranet sites. Not for electronic distribution.

TRIAL MODE − a valid license will remove this message. See the keywords property of this PDF for more information.

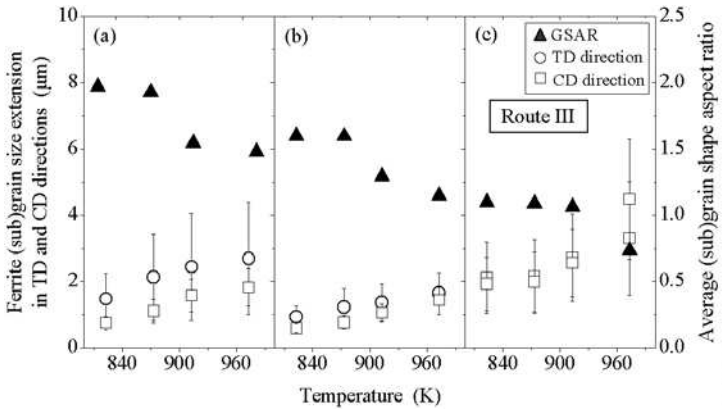

Fig. 4. Average grain and subgrain sizes of the ferrite. (a) Crystals surrounded by boundaries in the range $63° > \theta \geq 15°$; (b) crystals surrounded by boundaries in the range $63° > \theta \geq 2°$; (c) crystals surrounded by boundaries in the range $15° > \theta \geq 2°$. The right-hand ordinate indicates the corresponding values for the grain size aspect ratios (GSAR), data are taken from route III.

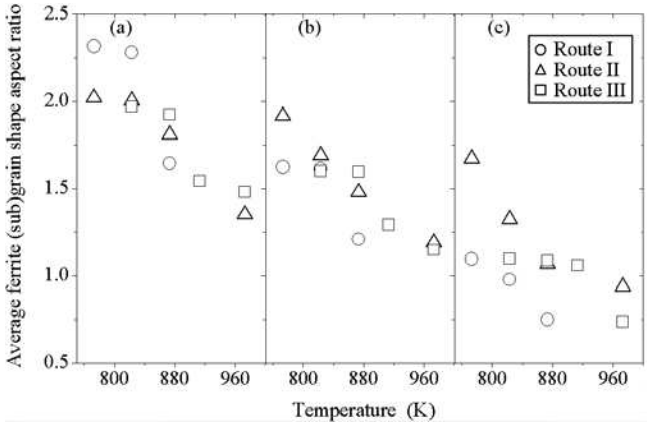

Fig. 5. Average values for the grain shape aspect ratios (GSAR). Data are taken for routes I, II, and III. (a) Crystals surrounded by boundaries in the range $63° > \theta \geq 15°$; (b) crystals surrounded by boundaries in the range $63° > \theta \geq 2°$; (c) crystals surrounded by boundaries in the range $15° > \theta \geq 2°$.

The dispersed globular cementite particles appear in both microstructures due to the effect of the large strain deformation. Most of the cementite particles are distributed on the ferrite grain boundaries and act as obstacles to grain boundaries migration. The pronounced alignment of cementite particles can be explained in terms of their position on the rims of the elongated ferrite grains.

This effect also explains the elongation of the ferrite grains even after recrystallization and subsequent growth, especially at lower deformation temperatures (Figs. 4, 5). At higher deformation/annealing temperatures the cementite particles may coarsen significantly, especially the particles located at grain boundary triple points.

4. Conclusions

The grain size is one of the most important microstructure parameters of steels. Therefore, it is important to measure it accurately. Particularly, steels produced by large-strain plastic deformation can have a high fraction of low-angle grain boundaries. Since these are known to be much less efficient for obtaining good mechanical properties than high-angle grain boundaries, it is important to separate the two when determining grain and subgrain sizes. In this study we investigated average ultrafine ferrite grains (0.9–2.2 μm), subgrains (0.6–1.5 μm), and cementite particles for three different processing routes in a plain C–Mn steel with 0.3 % carbon. The microstructures were investigated in terms of high-resolution EBSD maps in order to obtain satisfying statistics and good lateral resolution at the same time. High-angle grain boundaries occupied a large fraction (55–70 %) of the microstructure. The grain sizes were defined according to their misorientation angle. By using a novel combination of EBSD map analysis and the mean linear intercept method the sizes of grains and subgrains were separately obtained. We observed that fine, aligned cementite particles with average diameters below 250 nm on the ferrite grain boundaries acted as obstacles to ferrite grain growth at lower temperatures, which leads to slightly elongated ultrafine ferrite grains with a certain stability against further grain growth. Higher temperatures result in coarser cementite particles (250–950 nm) with a weaker pinning effect on the grain boundaries, resulting in more equiaxed ferrite grains.

The authors would like to express their gratitude to Dr. S. Zaefferer and Dr. N. Chen for helpful discussions. The financial support of the European Community for Steel and Coal (ECSC) is gratefully acknowledged.

References

[1] Y. Fukuda, K. Oh-ishi, Z. Horita: Acta Mater. 50 (2002) 1359.
[2] J. Kim, I. Kim, D.H. Shin: Scripta Mater. 45 (2001) 421.
[3] W.Y. Choo, K.K. Um: Ultrafine Grained Steels (ISUGS 2001) Fukuoka, Japan (2001) 156.
[4] Y.Q.Weng: Ultra-Steel 2000, Tsukuba, Japan (2000) 11.
[5] D.H. Shin, I. Kim, J. Kim: Acta Mater. 49 (2001) 1359.
[6] D.H. Shin, C.W. Seo, J.R. Kim: Scripta Mater. 42 (2000) 695.
[7] D.H. Shin, B.C. Kim, K.T. Park: Acta Mater. 48 (2000) 2247.
[8] D. Raabe: Steel Research 66 (1995) 222.
[9] M. Hölscher, D. Raabe, K. Lücke: Steel Research 62 (1991) 567.
[10] D. Raabe, F. Roters, V. Marx: Textures Microstruct. 26–27 (1996) 611.
[11] N. Tsuji, R. Ueji, Y. Minamino: Scripta Mater. 47 (2002) 69.
[12] M.C. Kim, Y.J. Oh, J.H. Hong: Scripta Mater. 43 (2000) 205.
[13] S. Zaefferer, J.C. Kuo, Z. Zhao, M. Winning, D. Raabe: Acta Mater. 51 (2003) 4719.
[14] R.Z. Valiev, I.V. Alexandrov: Ann. Chim. Sci. Mat*er.* 27 (2002) 3.
[15] A. Gholinia, P.B. Prangnell, M.V. Markushey: Acta Mater. 48 (2000) 1115.
[16] J.C. Glez, J.H.Driver: Acta Mater. 51 (2003) 2989.
[17] A. Gholinia, F.J. Humphreys, P.B. Prangnell: Acta Mater. 50 (2002) 4461.
[18] P.J. Apps, J.R. Bowen, P.B. Prangnell: Acta Mater. 51 (2003) 2811.
[19] P.J. Hurley, F.J. Humphreys: Acta Mater. 51 (2003) 1087.
[20] J. Wang, M. Furukawa, Z. Horita: Mater. Sci. & Eng. A 216 (1996) 41.
[21] K.T. Park, D.H. Shin: Mater.Sci. & Eng. A334 (2002) 79.
[22] B. Jansson, M. Schalin, B. Sundman: Phase Equilibria 14 (1993) 557.
[23] R. Kaspar, O. Pawelski: Materialprüfung 31 (1989) 14.

(Received November 5, 2003; accepted February 19, 2004)

Correspondence address

Prof. Dr.-Ing. D. Raabe
Max-Planck-Institut für Eisenforschung
Max-Planck-Str. 1, D-40237 Düsseldorf, Germany
Tel.: +49 211 679 2278
Fax: +49 211 679 2333
E-mail: raabe@mpie.de

© 2004 Carl Hanser Verlag, Munich, Germany www.hanser.de/mk Not for use in internet or intranet sites. Not for electronic distribution.

TRIAL MODE − a valid license will remove this message. See the keywords property of this PDF for more information.